Theor Chim Acta (1992) 82: 29–46

Theoretica Chimica Acta

A molecular theory of inhomogeneous broadening, including the correlation between different transitions, in liquids and glasses

H. M. Sevian and J. L. Skinner

Department of Chemistry and Theoretical Chemistry Institute, University of Wisconsin, Madison, WI 53706, USA

Received January 5, 1991; received in revised form February 19, 1991/Accepted May 20, 1991

Summary. We present a molecular theory of the energy distributions for the internal quantum states of a solute in a liquid or glassy solvent. We show that the energy distributions for different states are correlated in a way that depends on the solute-solvent interactions. We show how the theory can be modified easily to describe the transition-energy distributions for different pairs of states, which are of course related to inhomogeneously broadened absorption spectra. We also show that the distributions for different transitions are correlated, and describe how this correlation is measured by nonresonant fluorescence- and phosphorescence-line-narrowing and hole-burning experiments. The theory provides a microscopic framework within which to interpret different phenomenological models. For the case of a Lennard-Jones solute in a Lennard-Jones liquid solvent, we compare our theory to Monte Carlo simulation.

Key words: Inhomogeneous broadening – Solute-solvent interactions – Transition-energy distributions – Nonlinear spectroscopy

1. Introduction

Inhomogeneous broadening is ubiquitous in condensed phase spectroscopy. If we consider the transition between two distinct quantum states of a dilute impurity ("solute") molecule or atom, different solutes will experience different environments, producing different transition energies. The ensemble of these solutes then leads to the observed "inhomogeneously" broadened absorption lineshape. For a transition to be truly inhomogeneously broadened, the environment of each solute must be static on the relevant experimental time scale. In reality, however, there are always time-dependent fluctuations of the environments due to the thermal motion of the host molecules ("solvent"). In the absence of spectral diffusion (such that a suitably defined time average of the transition energy for a particular solute does not drift on the experimental timescale), if we assume that these fluctuations are (statistically) the same for each solute, they produce what is known as pure dephasing, which, coupled with any population relaxation, leads to homogeneous broadening [1–3]. The observed spectrum is then a

convolution of this homogeneous lineshape with the inhomogeneous transition energy distribution.

For many solute/solvent systems, especially at low temperatures, where the solvent is a crystalline or amorphous solid, the inhomogeneous distribution is much broader than the homogeneous lineshape, and so the observed lineshape is completely dominated by the former effect. This has prompted spectroscopists interested in condensed phase dynamics to develop techniques such as hole burning [4–7], fluorescence line narrowing (FLN) [8, 9], and photon echoes [10, 11], that enable one to determine the homogeneous lineshape even in those situations that are overwhelmingly inhomogeneously broadened. The spectacular success of these techniques has led naturally to the attitude that, like Doppler broadening in the gas phase and magnetic field inhomogeneities in NMR, inhomogeneous broadening is an unwanted complication in condensed phase spectroscopy.

Recent interest in the structure of disordered systems has refocused attention on the inhomogeneous transition energy distribution. By considering the energy distributions of the two quantum levels, one can imagine two extreme scenarios, each of which produces inhomogeneous broadening. In the first, one assumes that all solutes that have a certain energy in one quantum state are also degenerate in the other state. In other words, the conditional probability that if a solute has energy E in state α it has energy E' in state β is a delta function, and the two energy distributions are completely correlated. If the energy distributions of the two states have, for example, different widths, this necessarily leads to inhomogeneous broadening. In the other extreme scenario one assumes that the conditional probability discussed above is simply equal to the β state energy distribution. That is, the probability of obtaining energy E' in state β is independent of what the energy is in state α, which clearly produces inhomogeneous broadening. Moreover, the joint probability for finding E in state α and E' in state β factors into a product of the individual state distributions, and so the distributions are completely uncorrelated. These two possibilities, as well as the intermediate case of partial correlation, have been described with phenomenological models by Williamson and Kwiram [12], Selzer [13], Lee, Walsh and Fayer [14], and Suter et al. [15].

Since each of these extreme scenarios leads to inhomogeneous broadening, if an absorption spectrum is observed to be inhomogeneously broadened, it cannot be deduced which, if either, of the scenarios is valid for a particular experiment. On the other hand, if two (or more) different transitions are simultaneously probed, as in some FLN, phosphorescence-line-narrowing (PLN) and hole-burning studies, one can begin to unravel the extent to which different states, or more accurately, different transitions (see the discussion by Friedrich and Haarer [16]), are correlated. Indeed, all of these types of experiments [14–21] have been analyzed within the above phenomenological framework.

While this framework has provided us with considerable conceptual understanding, ultimately, inhomogeneous broadening is produced by microscopic interactions, and one would therefore like to couch the phenomenological ideas within a microscopic theory. A microscopic theory of the inhomogeneous lineshape of impurities in crystals was reviewed by Stoneham [22], which was later extended to consider the correlation between different transitions by Kikas and Rätsep [23]. Independent of the latter work, a related molecular theory directed toward crystalline or amorphous solids, which focused specifically on the conditional probabilities between states, was recently outlined by Laird and

Skinner [24]. Similar work on the absorption lineshape of a solute in a liquid solvent was performed by Loring [25]. Soon thereafter, Simon et al. [26] addressed in somewhat greater depth the question, for liquid solvents, of the energy distributions themselves. Along complementary lines, a recent computer simulation [27] shows [28] that for a realistic model of a solute in an amorphous solid the conditional probability is in the intermediate correlation regime.

The basic idea behind the microscopic theories of inhomogeneous broadening is that the energy levels of a dilute solute in a condensed phase are perturbed by a summation of pairwise interactions. For example, to understand the spectra of substitutional impurities in crystals [22, 23], one begins with a reference state of a single impurity in a perfect crystal. Various kinds of defects from an otherwise perfect crystal lattice then perturb these reference levels, and the actual distribution of levels for a particular state is obtained by performing an ensemble average of the different environments produced by different static defect configurations. For impurities in amorphous solids or liquids, the reference state of the perfect crystal is not particularly appropriate, and so instead we adopt the isolated solute in the gas phase as the relevant reference state [24, 26]. In this case the perturbations of the solute levels involve the interaction of the solute with all solvent atoms or molecules.

In what follows we focus specifically on the problem of structurally disordered solvents (liquids or glasses), although the formal theory is also applicable to crystals. In considering liquid solvents we realize that solute spectra are often not dominated by inhomogeneous broadening, due to rapid motion of the solvent. In glasses, however, since large-amplitude molecular motion is absent, solute spectra are indeed inhomogeneously broadened. Since the structure of liquids is very similar to that of glasses, the energy distributions and conditional probabilities that emerge from the liquid problem will be relevant to the amorphous solid solvent as well. Moreover, since the liquid is an equilibrium system, analytical theories of its structure, and computer simulation of solute spectra are more straightforward than for a glass. Therefore, our motivation for studying liquids is primarily to illuminate the situation in glasses.

In this paper we present a complete derivation of the energy level distributions and the conditional probabilities discussed by Laird and Skinner [24]. We then extend the theory of the conditional probabilities by incorporating solvent correlation, as discussed by Simon et al. [26] in their theory of the level distributions. We show that the phenomenological concepts and models discussed earlier are produced naturally by this microscopic theory. In Sect. 2 we present the theoretical derivations. In Sect. 3 we test the theory by performing Monte Carlo simulations for a particular molecular model – that of a Lennard-Jones solute in a Lennard-Jones liquid solvent. In Sect. 4 we show how the basic theory can be modified to describe various types of spectroscopic experiments involving two different transitions, and we compare our results to simulation. In Sect. 5 we conclude.

2. Microscopic derivation of single state and joint energy distributions

We consider a single solute atom or molecule in a static solvent, which could be an equilibrium liquid or crystal, or a nonequilibrium amorphous solid. However, we choose as a reference state the solute in the gas phase, which means, as discussed in the Introduction, that here we will focus specifically on spectroscopy

in liquids and glasses. We will assume that for each quantum state of the solute the interactions between solute and solvent can be decomposed in a pairwise-additive manner. We will further assume for simplicity that these pairwise interactions depend only on the distance between the solute and solvent molecules, although this assumption could very easily be relaxed. If we take the position of the solute to be the origin, then for a given configuration of N solvent atoms, the energy of state α of the solute is:

$$E_\alpha(\vec{R}_1, \ldots, \vec{R}_N) = E_\alpha^0 + \sum_{i=1}^{N} v_\alpha(R_i), \tag{2.1}$$

where E_α^0 is the unperturbed energy of the solute in state α, $\vec{R}_i$ is the position of the ith solvent molecule, R_i is its magnitude, and $v_\alpha(R)$ is the pairwise solute-solvent interaction potential for state α.

Assuming that only the ground state ($\alpha = 0$) of the solute is thermally populated, for an equilibrium liquid the distribution of solvent coordinates is given by:

$$P(\vec{R}_1, \ldots, \vec{R}_N) = \frac{V^N}{Z} \exp\left\{-\beta\left[\sum_i v_0(R_i) + U_s(\vec{R}_1, \ldots, \vec{R}_N)\right]\right\}, \tag{2.2}$$

$$Z = \int d\vec{R}_1 \cdots d\vec{R}_N \exp\left\{-\beta\left[\sum_i v_0(R_i) + U_s(\vec{R}_1, \ldots, \vec{R}_N)\right]\right\}, \tag{2.3}$$

where $\beta = 1/kT$, V is the volume of the system, and $U_s(\vec{R}_1, \ldots, \vec{R}_N)$ is the total solvent-solvent interaction potential energy. On the other hand, for a nonequilibrium glass, one cannot write down a simple expression for $P(\vec{R}_1, \ldots, \vec{R}_N)$, which is determined by the thermal history of the system. In either case, $P(\vec{R}_1, \ldots, \vec{R}_N)$ is normalized by:

$$\int d\vec{R}_1 \cdots d\vec{R}_N P(\vec{R}_1, \ldots, \vec{R}_N) = V^N. \tag{2.4}$$

Once the solute-solvent interaction and $P(\vec{R}_1, \ldots, \vec{R}_N)$ have been specified, the energy distribution of the solute in state α is given by:

$$\begin{aligned} p_\alpha(E) &= \frac{1}{V^N} \int d\vec{R}_1 \cdots d\vec{R}_N P(\vec{R}_1, \ldots, \vec{R}_N) \delta(E - E_\alpha(\vec{R}_1, \ldots, \vec{R}_N)) \\ &\equiv \langle \delta(E - E_\alpha(\vec{R}_1, \ldots, \vec{R}_N)) \rangle. \end{aligned} \tag{2.5}$$

Replacing the δ function with its integral representation yields:

$$p_\alpha(E) = \frac{1}{2\pi V^N} \int_{-\infty}^{\infty} dt e^{i(E - E_\alpha^0)t} \int d\vec{R}_1 \cdots d\vec{R}_N P(\vec{R}_1, \ldots, \vec{R}_N) e^{-i\sum_i v_\alpha(R_i)t}. \tag{2.6}$$

Following the method of Stoneham [22, 24, 29], we first make the assumption that the coordinates of the solvent molecules are uncorrelated. This means that the distribution function $P(\vec{R}_1, \ldots, \vec{R}_N)$ factors into the product of N two-particle solute-solvent radial distribution functions:

$$P(\vec{R}_1, \ldots, \vec{R}_N) = g(R_1) g(R_2) \cdots g(R_N). \tag{2.7}$$

This factorization is in the spirit of a mean-field-like approximation. Since it does not reflect an explicit consideration of solvent-solvent interactions, it is only

strictly valid for very low solvent densities. Applying this approximation, Eq. (2.6) becomes:

$$p_\alpha(E) = \frac{1}{2\pi}\int_{-\infty}^{\infty} dt e^{i(E-E_\alpha^0)t}\left[\frac{1}{V}\int d\vec{R} g(R) e^{-iv_\alpha(R)t}\right]^N. \tag{2.8}$$

Defining a new function $J_\alpha(t)$ by:

$$J_\alpha(t) = \int d\vec{R} g(R)[1 - e^{-iv_\alpha(R)t}], \tag{2.9}$$

taking the limit $N \to \infty$ while keeping the solvent density $\varrho = N/V$ constant, and recalling the relation, $\lim_{N\to\infty}[1 + x/N]^N = e^x$, results in:

$$p_\alpha(E) = \frac{1}{2\pi}\int_{-\infty}^{\infty} dt e^{i(E-E_\alpha^0)t} e^{-\varrho J_\alpha(t)}. \tag{2.10}$$

This result [22] can be applied to many situations of inhomogeneous broadening.

In general, this integral cannot be evaluated analytically. However, a simple approximation [24, 29] leads to a more tractable form: for large enough ϱ, the integrand in Eq. (2.10) is dominated by values of t for which $J_\alpha(t)$ is well-approximated by the first two terms in its Taylor expansion about $t = 0$:

$$J_\alpha(t) \approx i\int d\vec{R} g(R) v_\alpha(R) t + \tfrac{1}{2}\int d\vec{R} g(R) v_\alpha(R)^2 t^2. \tag{2.11}$$

Substituting this expansion into Eq. (2.10) and integrating yields a Gaussian expression in E:

$$p_\alpha(E) = \frac{1}{\sqrt{2\pi D_{\alpha\alpha}}}\exp\left[-\frac{(E-E_\alpha)^2}{2D_{\alpha\alpha}}\right], \tag{2.12}$$

centered at

$$E_\alpha = E_\alpha^0 + \varrho\int d\vec{R} g(R) v_\alpha(R), \tag{2.13}$$

and with variance

$$D_{\alpha\alpha} = \varrho\int d\vec{R} g(R) v_\alpha(R)^2. \tag{2.14}$$

The center energy of the Gaussian is the unperturbed energy plus a "solvent shift," which is simply related to the average solute-solvent interaction.

In the same spirit, the joint probability distribution for two solute quantum states may be derived. The probability that the solute has energy E in state α and energy E' in state β is given by:

$$p_{\alpha\beta}(E, E') = \langle \delta(E - E_\alpha(\vec{R}_1, \ldots, \vec{R}_N))\delta(E' - E_\beta(\vec{R}_1, \ldots, \vec{R}_N))\rangle. \tag{2.15}$$

Replacing the δ functions by their integral representations and following the procedure outlined above, the probability function becomes:

$$p_{\alpha\beta}(E, E') = \frac{1}{4\pi^2}\int_{-\infty}^{\infty} dt \int_{-\infty}^{\infty} dt' e^{i(E-E_\alpha^0)t} e^{i(E'-E_\beta^0)t'} e^{-\varrho J_{\alpha\beta}(t,t')}, \tag{2.16}$$

where

$$J_{\alpha\beta}(t, t') = \int d\vec{R} g(R)[1 - e^{-iv_\alpha(R)t} e^{-iv_\beta(R)t'}]. \tag{2.17}$$

Substituting the two-variable Taylor expansion for $J_{\alpha\beta}(t, t')$ about $t = t' = 0$, and performing the integrations in Eq. (2.16) gives:

$$p_{\alpha\beta}(E, E') = \frac{1}{2\pi\sqrt{(D_{\alpha\alpha}D_{\beta\beta} - D_{\alpha\beta}^2)}} \times \exp\left[-\frac{D_{\alpha\alpha}(E' - E_\beta)^2 - 2D_{\alpha\beta}(E' - E_\beta)(E - E_\alpha) + D_{\beta\beta}(E - E_\alpha)^2}{2(D_{\alpha\alpha}D_{\beta\beta} - D_{\alpha\beta}^2)} \right], \tag{2.18}$$

where

$$D_{\alpha\beta} = \varrho \int d\vec{R} g(R) v_\alpha(R) v_\beta(R). \tag{2.19}$$

The conditional probability that if the solute has energy E in state α it has energy E' in state β is defined by:

$$f_{\beta\alpha}(E' \mid E) = \frac{p_{\alpha\beta}(E, E')}{p_\alpha(E)}, \tag{2.20}$$

and from Eqs. (2.12) and (2.18) we see that it is a Gaussian in E':

$$f_{\beta\alpha}(E' \mid E) = \frac{1}{\sqrt{2\pi(D_{\beta\beta} - D_{\alpha\beta}^2/D_{\alpha\alpha})}} \exp\left[-\frac{(E' - E_\beta - (D_{\alpha\beta}/D_{\alpha\alpha})(E - E_\alpha))^2}{2(D_{\beta\beta} - D_{\alpha\beta}^2/D_{\alpha\alpha})} \right]. \tag{2.21}$$

Two interesting limits of this equation may be explored. First, in the limit that $D_{\alpha\alpha}D_{\beta\beta} = D_{\alpha\beta}^2$, $f_{\beta\alpha}(E' \mid E)$ becomes a delta function. From a microscopic perspective, this occurs, for example, when $v_\beta(R)/v_\alpha(R) = \lambda$ (a constant), and one finds that $f_{\beta\alpha}(E' \mid E) = \delta(E' - E_\beta - \lambda(E - E_\alpha))$. This corresponds to the phenomenological model discussed by Selzer [13], where it is assumed that there is a one-to-one correspondence between the energies in two different states. In the other extreme is the limit that $D_{\alpha\beta} \ll D_{\alpha\alpha}, D_{\beta\beta}$; in this case the conditional probability approaches the energy distribution of the β level, $p_\beta(E')$. (In this limit it is also easy to see that $p_{\alpha\beta}(E, E') \approx p_\alpha(E)p_\beta(E')$.) This corresponds to the model discussed by Lee, Walsh, and Fayer [14], in which it is assumed that there is no correlation between the energy of one state and the energy of another. The more general case of partial correlation has been described phenomenologically by Suter et al. [15]. Thus our theory illuminates the microscopic origin of these phenomenological models, and for any particular microscopic model of inhomogeneous broadening, shows how to determine the appropriate expression for the conditional probability.

A quantitative measure of the correlation between the two energy distributions is given by the ratio of the width of the conditional probability distribution $f_{\beta\alpha}(E' \mid E)$ to the width of the β state distribution:

$$R_{\beta\alpha} = \sqrt{1 - \frac{D_{\alpha\beta}^2}{D_{\alpha\alpha}D_{\beta\beta}}}. \tag{2.22}$$

Note that since $D_{\alpha\beta} = D_{\beta\alpha}$, $R_{\alpha\beta} = R_{\beta\alpha}$. From the Schwartz inequality that follows from Eq. (2.19), $D_{\alpha\beta}^2 \leqslant D_{\alpha\alpha} D_{\beta\beta}$, we see that $0 \leqslant R_{\beta\alpha} \leqslant 1$. Indeed, $R_{\beta\alpha} = 0$ and 1 correspond to the correlated and uncorrelated limits respectively.

In a similar manner as the derivation of Eq. (2.18) from Eq. (2.15), the triple joint probability may be derived from:

$$p_{\alpha\beta\gamma}(E, E', E'') = \langle \delta(E - E_\alpha(\vec{R}_1, \ldots, \vec{R}_N)) \times \delta(E' - E_\beta(\vec{R}_1, \ldots, \vec{R}_N)) \delta(E'' - E_\gamma(\vec{R}_1, \ldots, \vec{R}_N)) \rangle, \quad (2.23)$$

which can be generalized immediately to higher-order joint probabilities if desired.

In the above there are two assumptions that involve the solvent density. The first is that the solvent coordinates are uncorrelated, which is only strictly valid at low densities. The second is that the density is large enough that $e^{-\varrho J_\alpha(t)}$ is well-approximated by Taylor expanding $J_\alpha(t)$ about $t = 0$. It is not immediately obvious for what range of density this pair of assumptions holds. In fact, Monte Carlo simulations with a Lennard-Jones solute-solvent interaction at typical liquid densities (see below, and also the work of Simon et al. [26]) show that for the energy level distributions, while the theory models the simulation data qualitatively, it is quantitatively incorrect. Specifically, while the distributions are approximately Gaussian and the theory predicts the distribution centers accurately, it does not predict the variances well.

One way to correct this problem, which has been implemented by Simon et al. [26], is to retain some solvent-solvent correlation at the level of the three-particle (solute-solvent-solvent) distribution function, and then make the Kirkwood superposition approximation. For the Lennard-Jones solute-solvent interaction this scheme is shown to be reasonably accurate for the energy level distributions [26]. To derive these results we rewrite the energy distribution in Eq. (2.6) as:

$$p_\alpha(E) = \frac{1}{2\pi} \int_{-\infty}^{\infty} dt e^{i(E - E_\alpha^0)t} \langle e^{-i \sum_i v_\alpha(R_i) t} \rangle. \quad (2.24)$$

Performing a cumulant expansion of the term in brackets and truncating at second order gives:

$$\ln \langle e^{-i \sum_i v_\alpha(R_i) t} \rangle = -i \left\langle \sum_i v_\alpha(R_i) \right\rangle_c t - \frac{1}{2} \left\langle \left[\sum_i v_\alpha(R_i) \right]^2 \right\rangle_c t^2, \quad (2.25)$$

where the first and second cumulants are defined by $\langle X \rangle_c \equiv \langle X \rangle$ and $\langle X^2 \rangle_c \equiv \langle X^2 \rangle - \langle X \rangle^2$ [30]. Substituting this back into Eq. (2.24) and integrating over t we obtain a Gaussian expression for the energy distribution identical in form to Eq. (2.12), but with:

$$E_\alpha = E_\alpha^0 + \left\langle \sum_i v_\alpha(R_i) \right\rangle_c \quad (2.26)$$

and

$$D_{\alpha\alpha} = \left\langle \left[\sum_i v_\alpha(R_i) \right]^2 \right\rangle_c. \quad (2.27)$$

Using the definition of the two-particle solute-solvent correlation function, which because of isotropic potential interactions is simply the radial distribution function:

$$g(R_1) = \frac{1}{V^{N-1}} \int d\vec{R}_2 \cdots d\vec{R}_N P(\vec{R}_1, \ldots, \vec{R}_N), \tag{2.28}$$

and realizing that $\langle \sum_i v_\alpha(R_i) \rangle = N \langle v_\alpha(R_1) \rangle$, yields for the first cumulant:

$$\left\langle \sum_i v_\alpha(R_i) \right\rangle_c = \varrho \int d\vec{R} g(R) v_\alpha(R), \tag{2.29}$$

which shows that Eq. (2.26) is identical to Eq. (2.13). Similarly, using the definition of the three-particle solute-solvent-solvent correlation function:

$$g_3(\vec{R}_1, \vec{R}_2) = \frac{1}{V^{N-2}} \int d\vec{R}_3 \cdots d\vec{R}_N P(\vec{R}_1, \ldots, \vec{R}_N), \tag{2.30}$$

and the fact that:

$$\left\langle \sum_{ij} v_\alpha(R_i) v_\alpha(R_j) \right\rangle = N \langle v_\alpha(R_1)^2 \rangle + N(N-1) \langle v_\alpha(R_1) v_\alpha(R_2) \rangle, \tag{2.31}$$

then in the limit $N \to \infty$ the variance becomes:

$$D_{\alpha\alpha} = \varrho \int d\vec{R} g(R) v_\alpha(R)^2 + \varrho^2 \int d\vec{R}\, d\vec{R}' v_\alpha(R) v_\alpha(R') [g_3(\vec{R}, \vec{R}') - g(R) g(R')]. \tag{2.32}$$

The first term in this equation is identical to Eq. (2.14), but there is an additional term proportional to density squared that involves the triplet correlation function. Following Simon et al. [26], we make use of the Kirkwood superposition approximation:

$$g_3(\vec{R}_1, \vec{R}_2) \approx g(R_1) g(R_2) g_s(|\vec{R}_1 - \vec{R}_2|), \tag{2.33}$$

where $g_s(R)$ is the solvent-solvent radial distribution function (which we assume also depends only on the solvent-solvent distance), to give:

$$D_{\alpha\alpha} = \varrho \int d\vec{R} g(R) v_\alpha(R)^2 + \varrho^2 \int d\vec{R}\, d\vec{R}' v_\alpha(R) v_\alpha(R') g(R) g(R') [g_s(|\vec{R} - \vec{R}'|) - 1]. \tag{2.34}$$

Notice that if we take the solvent-solvent distribution function to be 1, i.e., no solvent-solvent correlation, then Eq. (2.14) is recovered. Since the second term in Eq. (2.34) involves a convolution, it can be evaluated most easily with Fourier transforms [26].

In a similar manner we can incorporate solvent correlation into our theory of the joint probability distributions, and hence the conditional probabilities. Rewriting Eq. (2.15) as:

$$p_{\alpha\beta}(E, E') = \frac{1}{4\pi^2} \int_{-\infty}^{\infty} dt \int_{-\infty}^{\infty} dt' e^{i(E - E_\alpha^0)t} e^{i(E' - E_\beta^0)t'} \langle e^{-i[\sum_i v_\alpha(R_i)t + \sum_i v_\beta(R_i)t']} \rangle, \tag{2.35}$$

truncating the cumulant expansion of the term in brackets at second order, performing the t and t' integrations, and using the superposition approximation,

leads to a Gaussian expression for $p_{\alpha\beta}(E, E')$ identical in form to Eq. (2.18), and with E_α given by Eq. (2.13), but with:

$$D_{\alpha\beta} = \varrho \int d\vec{R} g(R) v_\alpha(R) v_\beta(R) + \varrho^2 \int d\vec{R}\, d\vec{R}' v_\alpha(R) v_\beta(R') g(R) g(R') [g_s(|\vec{R} - \vec{R}'|) - 1]. \tag{2.36}$$

Thus we see that upon including solvent-solvent correlations, the center energies of both the single state and joint probability distributions remain unchanged, but the widths are modified.

3. Conditional probabilities for a solute in a Lennard-Jones liquid

To illustrate the theory, and especially to show how different values of the correlation parameter $R_{\beta\alpha}$ are produced by different microscopic interactions, we consider the specific case of a Lennard-Jones solute in an equilibrium Lennard-Jones liquid solvent. The interaction between the solute in state α and the solvent is taken to be:

$$v_\alpha(R) = 4\epsilon_\alpha \left[\left(\frac{\sigma_\alpha}{R} \right)^{12} - \left(\frac{\sigma_\alpha}{R} \right)^{6} \right], \tag{3.1}$$

where σ_α is roughly interpreted as the sum of the radii of the solvent and the solute in state α, and ϵ_α is the well depth. The solvent-solvent interaction potential is given by:

$$v_s(R) = 4\epsilon \left[\left(\frac{\sigma}{R} \right)^{12} - \left(\frac{\sigma}{R} \right)^{6} \right]. \tag{3.2}$$

In order to obtain a crude understanding of how the Lennard-Jones parameters affect $R_{\beta\alpha}$, we first consider the simple approximation that:

$$g(R) = e^{-\beta v_0(R)}, \tag{3.3}$$

which can be obtained from Eqs. (2.2), (2.3) and (2.28) by neglecting entirely the solvent-solvent interaction. We then use only the first-order expression Eq. (2.19) to evaluate $D_{\alpha\beta}$. The result is [31]:

$$\begin{aligned} D_{\alpha\beta} = {} & \frac{2^{3/4}\pi^{3/2}}{48} \epsilon_\alpha \epsilon_\beta \varrho \sigma_0^3 (\beta\epsilon_0)^{-7/4} e^{\beta\epsilon_0/2} \left(\frac{\sigma_\alpha}{\sigma_0} \right)^6 \left(\frac{\sigma_\beta}{\sigma_0} \right)^6 \\ & \times \left\{ 15 \left(\frac{\sigma_\alpha}{\sigma_0} \right)^6 \left(\frac{\sigma_\beta}{\sigma_0} \right)^6 D_{-7/2}(-\sqrt{2\beta\epsilon_0}) \right. \\ & \left. - 12\sqrt{2\beta\epsilon_0} \left[\left(\frac{\sigma_\alpha}{\sigma_0} \right)^6 + \left(\frac{\sigma_\beta}{\sigma_0} \right)^6 \right] D_{-5/2}(-\sqrt{2\beta\epsilon_0}) + 32\beta\epsilon_0 D_{-3/2}(-\sqrt{2\beta\epsilon_0}) \right\}, \end{aligned} \tag{3.4}$$

where $D_\nu(x)$ is the parabolic cylinder function [32], which can be evaluated from tables or numerically. We see from the above and Eq. (2.22) that $R_{\beta\alpha}$ depends only on the three dimensionless ratios $\beta\epsilon_0$, σ_α/σ_0, and σ_β/σ_0.

Specifically focusing on the correlation between the ground state energy distribution and some excited state distribution, we take $\alpha = 0$ and $\beta = 1$. In

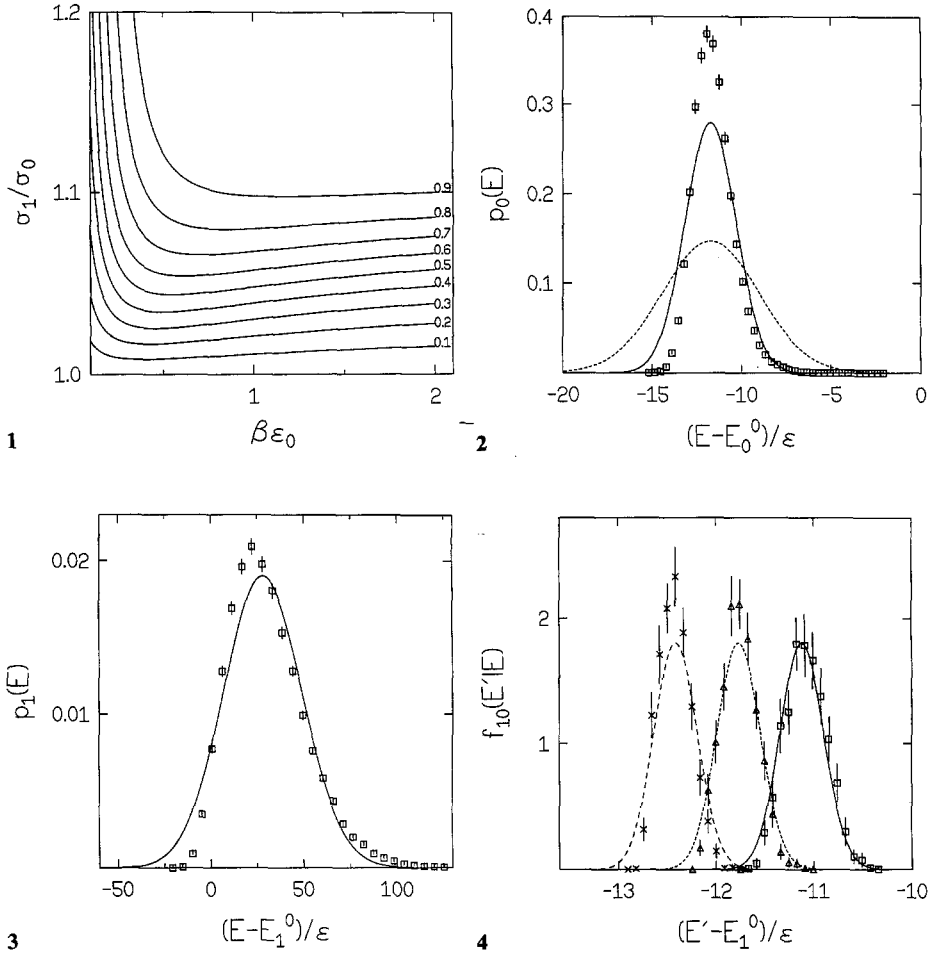

Fig. 1. The correlation parameter R_{10} as a function of the dimensionless ratios σ_1/σ_0 and $\beta\epsilon_0$, for the model discussed in the text. The solid lines are contours, with the values indicated

Fig. 2. $p_0(E)$ vs $(E - E_0^0)/\epsilon$. The *squares* with error bars are the simulation data, and the *dotted* and *solid lines* are from Eqs. (2.12), (2.13), and (2.14) and (2.34) respectively

Fig. 3. $p_1(E)$ vs $(E - E_1^0)/\epsilon$ for $\sigma_1/\sigma_0 = 1.20$. The *squares* are the simulation data, and the *solid line* is from Eqs. (2.12), (2.13), and (2.34)

Fig. 4. $f_{10}(E' \mid E)$ vs $(E' - E_1^0)/\epsilon$ for $\sigma_1/\sigma_0 = 1.01$. The *squares* and *solid line* correspond to $(E - E_0^0)/\epsilon = -11.14$, the *triangles* and *short dashed line* correspond to $(E - E_0^0)/\epsilon = -11.74$, and the $\times$'s and *long dashed line* correspond to $(E - E_0^0)/\epsilon = -12.34$

Fig. 1 is shown a contour plot of R_{10} as a function of $\beta\epsilon_0$ and σ_1/σ_0. For $\sigma_1/\sigma_0 = 1$, $v_1(R)/v_0(R) = \epsilon_1/\epsilon_0$, which is a constant, and so, as discussed earlier, $R_{10} = 0$. We see that in general, as σ_1/σ_0 increases, R_{10} increases, and for a reasonable range of dimensionless ratios σ_1/σ_0 and $\beta\epsilon_0$ one obtains the full range of R_{10} values. Thus both extreme limits of the conditional probabilities can be produced by the same form of the solute-solvent interaction potential.

Armed with a rough idea of what parameters to choose, in order to check quantitatively the theory we next present a Monte Carlo simulation of the full solute-solvent system introduced above. It is easy to see from Eqs. (2.22) and (2.19) or (2.36) that R_{10} does not depend on the value of ϵ_1, and we therefore set $\epsilon_1 = \epsilon_0$. To simplify matters further, we assume that $\sigma_0 = \sigma$ and $\epsilon_0 = \epsilon$, that is, in its ground state (which, as mentioned previously, we assume is the only state that is thermally populated) the solute interacts with solvent molecules in the same way that solvent molecules interact with each other. We implement this simplification in order to improve the statistics of the energy distributions, since in this way we can consider each particle in the fluid to be a solute; for an N particle Monte Carlo system, the statistics are improved $\sqrt{N}$-fold. We choose thermodynamic parameters so that the solvent is a liquid near the triple point [33]: $\varrho\sigma^3 = 0.81408$ and $1/\beta\epsilon = 0.7866667$.

In the Monte Carlo simulations we consider a canonical ensemble of 810 particles in a three-dimensional cubic box with periodic boundaries. All potential interactions are truncated at half the box length. In calculating the statistical error bars, which are always reported as two standard deviations, it is necessary to average over uncorrelated configurations, which from the fluctuations in $g(R)$ we determined to be every twelfth configuration. To calculate the energy distributions, for each uncorrelated configuration the solute energy is obtained from a pairwise sum of the appropriate solute-solvent potentials.

In Fig. 2 is shown the energy distribution of the solute in its ground state, $p_0(E)$. The data points are from the Monte Carlo simulation. The dashed line is calculated from Eqs. (2.12), (2.13), and (2.14), with the radial distribution function $g(R)$ taken from the simulation. As seen, although the center energy E_0 is obtained accurately, the variance D_{00} is quantitatively incorrect. A better approximation, shown as the solid line, comes from Eqs. (2.12), (2.13), and (2.34). Thus the incorporation of solvent-solvent correlation significantly improves the theory.

To calculate excited state energy distributions and conditional probabilities we need to choose values of σ_1/σ_0. To obtain values of R_{10} such that $R_{10} \ll 1$,

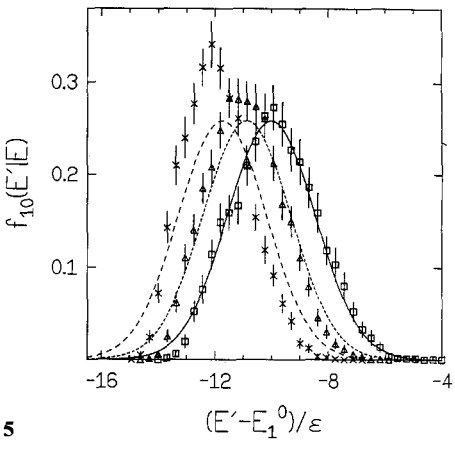

5

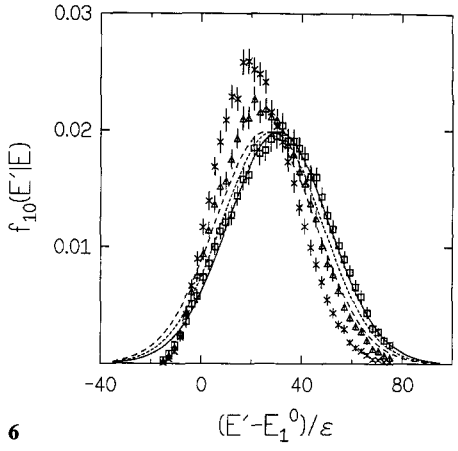

6

Fig. 5. Same as Fig. 4 but for $\sigma_1/\sigma_0 = 1.05$

Fig. 6. Same as Fig. 4 but for $\sigma_1/\sigma_0 = 1.20$

$R_{10} \approx 0.5$, and $R_{10} \approx 1$, which reflect very correlated, partially correlated, and nearly uncorrelated distributions respectively, we see from Fig. 1 that for the simulation (inverse) temperature of $\beta\epsilon_0 \approx 1.27$, suitable choices are $\sigma_1/\sigma_0 = 1.01$, 1.05, and 1.20. Indeed, calculation of R_{10} from Eqs. (2.22) and (2.36) with these choices (but using the $g(R)$ from simulation) yields $R_{10} = 0.146$, 0.602, and 0.949, respectively.

The excited state distribution, $p_1(E)$, for $\sigma_1/\sigma_0 = 1.20$ is shown in Fig. 3. The simulation data are in reasonable agreement with the theoretical result from Eqs. (2.12), (2.13), and (2.34). Similar results are obtained for the other values of σ_1/σ_0.

We also compare the simulation to theory for the conditional probability $f_{10}(E' \mid E)$ for the three ratios of σ_1/σ_0, and for three values of E, one near the center of the ground state distribution, $(E - E_0^0)/\epsilon = -11.74$, and one to each side of the center: $(E - E_0^0)/\epsilon = -11.14$ and -12.34. Conditional probabilities are calculated from Eqs. (2.13), (2.21), and (2.36). The comparisons for $\sigma_1/\sigma_0 = 1.01$, 1.05 and 1.20 are shown in Figs. 4, 5, and 6. The agreement between simulation and theory is not too bad, especially for the smaller values of σ_1/σ_0 or larger values of $(E - E_0^0)/\epsilon$.

To conclude this section, the Monte Carlo simulation shows that the simple molecular theory that takes into account solvent-solvent correlation, at least in a crude manner, provides a reasonably accurate description of the energy distributions and conditional probabilities. The simulation also verifies that this simple molecular model with a single form for the solute-solvent interaction, can, by simply changing the Lennard-Jones σ parameter, span the complete range of energy distribution correlation discussed phenomenologically by others.

4. Spectroscopy

Although energy distributions and the associated conditional probabilities are of fundamental interest, in spectroscopic experiments only *differences* between energy levels can be measured. The above microscopic theory can be extended to describe directly several different types of spectroscopy. The absorption spectrum, for example, is equal to a transition-energy probability distribution, while some FLN, PLN and hole-burning spectroscopies are related to two-point joint transition-energy distributions.

The probability distribution for the transition energy between states α and β can be calculated in much the same way as a simple energy distribution, beginning with

$$p_{\alpha\beta}(\Delta E) = \langle \delta(\Delta E - [E_\alpha(\vec{R}_1, \ldots, \vec{R}_N) - E_\beta(\vec{R}_1, \ldots, \vec{R}_N)]) \rangle. \tag{4.1}$$

Thus, as in Eq. (2.24), this can be written as:

$$p_{\alpha\beta}(\Delta E) = \frac{1}{2\pi} \int_{-\infty}^{\infty} dt e^{i(\Delta E - E_\alpha^0 + E_\beta^0)t} \langle e^{-i\sum_i v_{\alpha\beta}(R_i)t} \rangle, \tag{4.2}$$

where $v_{\alpha\beta}(R) = v_\alpha(R) - v_\beta(R)$. This yields a Gaussian expression in ΔE:

$$p_{\alpha\beta}(\Delta E) = \frac{1}{\sqrt{2\pi F_{\alpha\beta}}} \exp\left[-\frac{(\Delta E - E_{\alpha\beta})^2}{2F_{\alpha\beta}} \right], \tag{4.3}$$

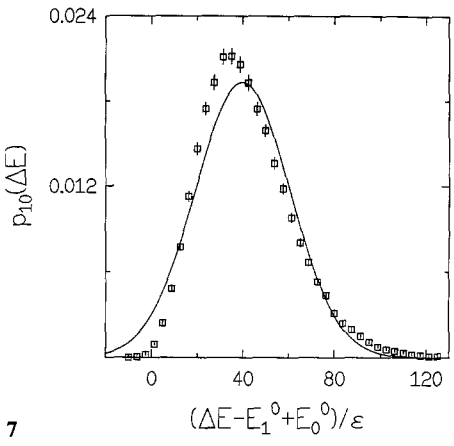

7

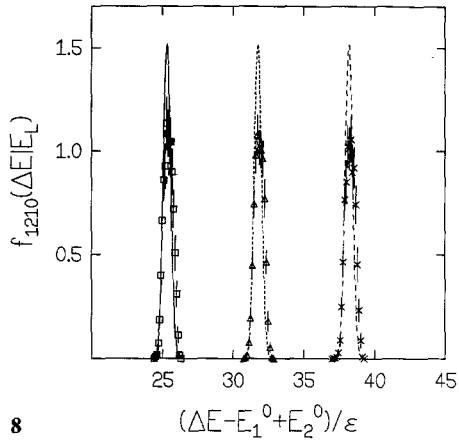

8

Fig. 7. The absorption spectrum $p_{10}(\Delta E)$ vs $(\Delta E - E_1^0 + E_0^0)/\epsilon$ for $\sigma_1/\sigma_0 = 1.20$. The *squares* are from the simulation and the *solid line* is from Eq. (4.3)

Fig. 8. The FLN conditional probability $f_{1210}(\Delta E \mid E_L)$ vs $(\Delta E - E_1^0 + E_2^0)/\epsilon$ for $\sigma_1/\sigma_0 = 1.20$ and $\sigma_2/\sigma_0 = 1.05$. The *squares* and *solid line* correspond to $(E_L - E_1^0 + E_0^0)/\epsilon = 25$, the *triangles* and *short dashed line* correspond to $(E_L - E_1^0 + E_0^0)/\epsilon = 32$, and the $\times$'s and *long dashed line* correspond to $(E_L - E_1^0 + E_0^0)/\epsilon = 39$

where

$$E_{\alpha\beta} = E_\alpha - E_\beta, \tag{4.4}$$

$$F_{\alpha\beta} = D_{\alpha\alpha} + D_{\beta\beta} - 2D_{\alpha\beta}. \tag{4.5}$$

In the uncorrelated limit, where $D_{\alpha\beta} \ll D_{\alpha\alpha}$, $D_{\beta\beta}$, one obtains a variance of $D_{\alpha\alpha} + D_{\beta\beta}$. In the case where $v_\beta(R)/v_\alpha(R) = \lambda$, we find a variance of $D_{\alpha\alpha}(\lambda - 1)^2$, which is nonzero when the α and β energy distributions have different widths ($\lambda \neq 1$). Thus we see that either of the extreme cases discussed earlier leads to inhomogeneous broadening.

This distribution can also be derived from:

$$p_{\alpha\beta}(\Delta E) = \int dE' \int dE p_{\alpha\beta}(E, E')\delta(\Delta E - [E - E']), \tag{4.6}$$

leading to the same results [24].

Turning to a quantitative check of the theory, we consider the inhomogeneous absorption lineshape for the transition from the solute ground state ($\beta = 0$) to some excited state ($\alpha = 1$), which is simply $p_{10}(\Delta E)$. In Fig. 7 we compare the predictions given by Eqs. (4.3, 4.4, 4.5, 2.13, and 2.36) for $p_{10}(\Delta E)$ to the Monte Carlo simulation for the case of $\sigma_1/\sigma_0 = 1.20$. The spectrum is quite broad and the theory models it reasonably well.

The joint probability distribution for a transition between states α and β, and a transition between states γ and δ, is given by:

$$p_{\alpha\beta\gamma\delta}(\Delta E, \Delta E') = \langle \delta(\Delta E - [E_\alpha(\vec{R}_1, \ldots, \vec{R}_N) - E_\beta(\vec{R}_1, \ldots, \vec{R}_N)]) \times \delta(\Delta E' - [E_\gamma(\vec{R}_1, \ldots, \vec{R}_N) - E_\delta(\vec{R}_1, \ldots, \vec{R}_N)]) \rangle. \tag{4.7}$$

The derivation follows the same course as that of the joint energy distribution in Sect. 2. The end result is:

$$p_{\alpha\beta\gamma\delta}(\Delta E, \Delta E') = \frac{1}{2\pi\sqrt{(F_{\alpha\beta}F_{\gamma\delta} - Q^2_{\alpha\beta\gamma\delta})}} \times \exp\left[-\frac{F_{\alpha\beta}(\Delta E' - E_{\gamma\delta})^2 - 2Q_{\alpha\beta\gamma\delta}(\Delta E - E_{\alpha\beta})(\Delta E' - E_{\gamma\delta}) + F_{\gamma\delta}(\Delta E - E_{\alpha\beta})^2}{2(F_{\alpha\beta}F_{\gamma\delta} - Q^2_{\alpha\beta\gamma\delta})}\right], \tag{4.8}$$

where

$$Q_{\alpha\beta\gamma\delta} = D_{\alpha\gamma} + D_{\beta\delta} - D_{\alpha\delta} - D_{\beta\gamma} = \tfrac{1}{2}(F_{\alpha\delta} + F_{\beta\gamma} - F_{\alpha\gamma} - F_{\beta\delta}). \tag{4.9}$$

These same results can also be derived, in principle, from the four-point joint distribution function:

$$p_{\alpha\beta\gamma\delta}(\Delta E, \Delta E') = \int dE''' \int dE'' \int dE' \int dE p_{\alpha\beta\gamma\delta}(E, E', E'', E''') \times \delta(\Delta E - [E - E'])\delta(\Delta E' - [E'' - E'']). \tag{4.10}$$

Note, however, that Eq. (6) of Ref. [24], which is related to a special case of the above, is incorrect, because the triple joint probability distribution does not factor into the product of the α energy distribution and the $\beta\alpha$ and $\gamma\beta$ conditional probabilities as indicated therein.

The conditional probability that if the solute has transition energy ΔE between states α and β it has transition energy $\Delta E'$ between states γ and δ is given by:

$$f_{\gamma\delta\alpha\beta}(\Delta E' \mid \Delta E) = \frac{1}{\sqrt{2\pi(F_{\gamma\delta} - Q^2_{\alpha\beta\gamma\delta}/F_{\alpha\beta})}} \times \exp\left[-\frac{(\Delta E' - E_{\gamma\delta} - (Q_{\alpha\beta\gamma\delta}/F_{\alpha\beta})(\Delta E - E_{\alpha\beta}))^2}{2(F_{\gamma\delta} - Q^2_{\alpha\beta\gamma\delta}/F_{\alpha\beta})}\right]. \tag{4.11}$$

The ratio of the width of this conditional probability to the width of the $\gamma\delta$ transition-energy distribution:

$$R_{\gamma\delta\alpha\beta} = \sqrt{1 - \frac{Q^2_{\alpha\beta\gamma\delta}}{F_{\alpha\beta}F_{\gamma\delta}}}, \tag{4.12}$$

is a measure of the correlation between transition-energy distributions.

In several different types of experiments, discussed below, this conditional probability can be measured directly. That is, the energy of the $\alpha\beta$ transition is laser-selected, and then the resulting $\gamma\delta$ energy distribution is determined. Therefore the ratio $R_{\gamma\delta\alpha\beta}$ is a quantitative indicator of the laser-selected narrowing of the $\gamma\delta$ distribution.

For example, in a typical fluorescence-line-narrowing experiment one excites an inhomogeneously broadened transition between two electronic levels with a narrow-band laser. One finds [17, 18] that fluorescence resonant with the laser is sharp, while nonresonant fluorescence (to an excited vibrational or crystal field level in the ground electronic state or to another excited electronic state) is less sharp, but still narrower than the nonresonant fluorescence that results from

broad-band excitation (which corresponds to the full inhomogeneous transition-energy distribution). Thus, in the former situation, the laser has already selected out a particular transition-energy difference between states that we will label 0 (ground) and 1 (excited), which is manifest in monochromatic fluorescence for this transition. On the other hand, fluorescence from level 1 to a third level, 2, is not necessarily constrained by the laser-prescribed 1-0 energy difference.

We can first consider the case of resonant fluorescence, where $\alpha = \gamma = 1$ and $\beta = \delta = 0$. From Eqs. (4.5), (4.9), and (4.12) we see that in this case, as expected, the ratio of the narrowed to unnarrowed fluorescence linewidths, R_{1010}, is zero, showing that with narrow-band laser excitation resonant fluorescence is sharp. For nonresonant fluorescence we have $\alpha = \gamma = 1$, $\beta = 0$ and $\delta = 2$. In the correlated limit where $v_1(R)/v_0(R) = \lambda$, and $v_2(R)/v_0(R) = \lambda'$ we find, again as expected, that $R_{1210} = 0$. Thus in the correlated limit one obtains complete line narrowing even for nonresonant transitions.

More generally, the nonresonant $1 \rightarrow 2$ fluorescence intensity is proportional to the conditional probability $f_{1210}(\Delta E \mid E_L)$, where E_L is the laser energy and ΔE is the fluorescence energy. In Fig. 8 is shown a comparison of the Monte Carlo data to the theory for this conditional probability for $\sigma_1/\sigma_0 = 1.20$ and $\sigma_2/\sigma_0 = 1.05$. Three different laser energies are shown, corresponding to the center of the 0-1 absorption spectrum, $(E_L - E_1^0 + E_0^0)/\epsilon = 32$, and one to each side of the center, $(E_L - E_1^0 + E_0^0)/\epsilon = 25$ and 39. For these parameters we calculate the ratio of this fluorescence linewidth to the full inhomogeneous linewidth for the $1 \rightarrow 2$ transition, finding that $R_{1210} = 0.0138$, which shows that the fluorescence is narrowed quite substantially compared to that resulting from broad-band excitation.

Narrowing effects similar to those found in FLN can also occur in phosphorescence spectroscopy. In this case one considers a solute with ground and excited singlet states, and a low-lying triplet state. When the triplet is directly excited with a narrow-band laser one obtains sharp phosphorescence, but when the singlet is excited, upon intersystem crossing the phosphorescence is broader [12, 15, 19, 20]. If the ground and excited singlet and triplet states are labeled 0, 1, and 2 respectively, then the phosphorescence spectrum after narrow-band singlet excitation is proportional to $f_{2010}(\Delta E \mid E_L)$. In Fig. 9 is compared the Monte Carlo simulation to the theory for the same values of σ_1, σ_2 and E_L as in Fig. 8. The phosphorescence is narrowed, but not as much as the fluorescence – our theoretical calculation gives $R_{2010} = 0.158$ for the ratio of the narrowed to broad-band excitation phosphorescence linewidths.

Hole-burning spectroscopy can also involve the correlation between two different transitions. In a photochemical hole-burning experiment, a transition between the ground state and a particular excited state of the solute is irradiated with a narrow-band laser. A certain fraction of the solutes reacts photochemically to form a new solute species, the photoproduct. Subsequently, the absorption profile of the solute is measured, resulting in a narrow hole at the laser frequency. In one interesting experiment [16] a narrow hole was burnt in a vibronic transition, which resulted in broader nonresonant holes at the electronic origin. The level scheme appropriate for this experiment is identical to the PLN scheme – in this case 0 is the ground state, 1 is the vibronic level, and 2 is the vibrationless excited electronic state. The nonresonant hole spectrum is again proportional to $f_{2010}(\Delta E \mid E_L)$.

The photoproduct in general absorbs at a different frequency from the solute, and so one can sometimes measure its absorption profile (the anti-hole), which

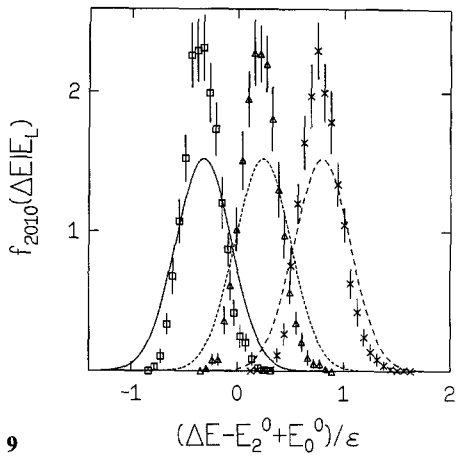

9

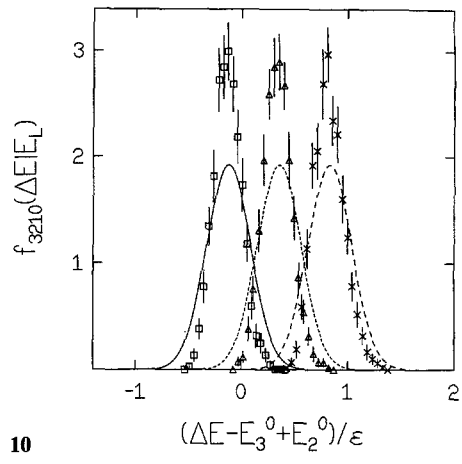

10

Fig. 9. The PLN conditional probability $f_{2010}(\Delta E \mid E_L)$ vs $(\Delta E - E_2^0 + E_0^0)/\epsilon$ for the same σ_1 and σ_2 and values of E_L as in Fig. 8

Fig. 10. The anti-hole conditional probability $f_{3210}(\Delta E \mid E_L)$ vs $(\Delta E - E_3^0 + E_2^0)/\epsilon$ for $\sigma_1/\sigma_0 = 1.20$, $\sigma_2/\sigma_0 = 1.01$, and $\sigma_3/\sigma_0 = 1.05$, and for the same values of E_L as in Fig. 8

is found to be substantially broader than the original hole [14, 21]. Thus this experiment measures the correlation between two completely distinct transitions (no common levels). If the ground and excited states of the solute are 0 and 1, and the ground and excited states of the photoproduct are 2 and 3, the anti-hole absorption spectrum is proportional to $f_{3210}(\Delta E \mid E_L)$. In Fig. 10 is shown the comparison between theory and simulation for this conditional probability, for $\sigma_1/\sigma_0 = 1.20$, $\sigma_2/\sigma_0 = 1.01$, and $\sigma_3/\sigma_0 = 1.05$, for three different values of E_L. In this case the ratio of the anti-hole width to the full photoproduct inhomogeneous linewidth is $R_{3210} = 0.146$.

5. Discussion

We have presented a simple molecular theory of the inhomogeneous energy distributions of the internal quantum states of a solute in a liquid or glassy solvent. These distributions, which are predicted to be Gaussian, are shown to be correlated with each other. We show how changing the solute-solvent interactions determines this level of correlation. We also show how the theory can be modified to describe spectroscopic observables. That is, we determine the transition-energy distributions for different pairs of levels, and show how these distributions are correlated. We then describe some applications of the theory to fluorescence-line-narrowing, phosphorescence-line-narrowing and hole-burning spectroscopies. This theory supplies a microscopic framework for the phenomenological models that have been discussed previously.

We have illustrated the theory with a simple model of a Lennard-Jones solute in a Lennard-Jones liquid solvent, and have shown that the theory compares quite favorably to Monte Carlo simulations of the same model. For other solute-solvent interactions, the Gaussian approximations may not be adequate, and one could extend the theory along the lines of the closest particle distribution approach of Simon et al. [26]. For a Lennard-Jones solute in a Lennard-

Jones glass, the results would be similar to that of the liquid solvent, since the solute-solvent radial distribution functions for the two cases are quite similar. For a quantitative comparison, it would be straightforward to implement one of several quenching techniques in order to generate the appropriate radial distribution function from computer simulation. In the derivation of the theory we have assumed isotropic solute-solvent and solvent-solvent interactions. As mentioned before, this assumption could be relaxed quite easily. Finally, many of the formal ideas espoused herein may be applicable to spectroscopy in crystalline solids as well.

In experiments that essentially measure the conditional probability between two different transitions, it is typically found that the narrowing observed from selective excitation of the first transition is less pronounced than that found in our Lennard-Jones model. For example, Suter et al. [15] measure the phosphorescence spectra of 1-indanones in different glasses upon both narrow-band and broad-band singlet excitation. They report linewidth ratios of the former to the latter in the range of 0.33–1. In contrast, in the single example of this type of experiment described in this paper we found a ratio of 0.16. Part of this difference is surely due to the unrealistic nature of our interaction potentials – indeed, the triplet solute-solvent interaction may be quite different in form from that of the singlet. There is also the possibility that for these (and other) relatively long-time-scale experiments, the solvent rearranges around the excited solute, leading to an additional source of broadening that is not treated in the present theory.

Note added in proof

Messing, Raz and Jortner [(1977) J Chem Phys 66:2239;4577] had previously derived expressions for the first two moments of the absorption lineshape that are completely equivalent to our Gaussian results. By making an exponential density expansion, they also showed how the theory can describe asymmetric lineshapes. JLS thanks Prof. Jortner for bringing this work to our attention.

Acknowledgements. JLS is greatly indebted to Joe Hirschfelder for his generosity in creating the Joseph O. Hirschfelder Professorship in Theoretical Chemistry, and for the atmosphere of excitement and creativity that pervades the Theoretical Chemistry Institute at the University of Wisconsin. The authors thank Jeffrey Saven for a critical reading of the manuscript. This research is supported by the National Science Foundation under grant nos. CHE89-10749 and CHE90-96272.

References

1. Skinner JL, Hsu D (1986) J Phys Chem 90:4931
2. Skinner JL (1988) Annu Rev Phys Chem 39:463
3. Silbey R, Kastner K (1987) J Luminescence 36:283
4. Small GJ (1983) In: Agranovich VM, Hochstrasser RM (eds) Spectroscopy and excitation dynamics of condensed molecular systems. North-Holland, Amsterdam
5. Haarer D, Silbey R (1990) Phys Today May, 58
6. Volker S (1989) Annu Rev Phys Chem 40:499
7. Volker S (1989) In: Funfschilling J (ed) Relaxation processes in molecular excited states. Kluwer Academic
8. Yen WM, Brundage RT (1987) J Luminescence 36:209
9. Weber MJ (1981) In: Yen WM, Selzer PM (eds) Laser spectroscopy of solids. Springer-Verlag, Berlin
10. Hesselink WH, Wiersma DA (1983) In: Agranovich VM, Hochstrasser RM (eds) Spectroscopy and excitation dynamics of condensed molecular systems. North-Holland, Amsterdam

11. Berg M, Walsh CA, Narasimhan LR, Littau KA, Fayer MD (1988) J Chem Phys 88:1564
12. Williamson RL, Kwiram AL (1979) J Phys Chem 83:3393
13. Selzer PM (1981) In: Yen WM, Selzer PM (eds) Laser spectroscopy of solids. Springer, Berlin Heidelberg New York
14. Lee HWH, Walsh CA, Fayer MD (1985) J Chem Phys 82:3948
15. Suter GW, Wild UP, Holzwarth AR (1986) Chem Phys 102:205
16. Friedrich J, Haarer D (1983) J Chem Phys 79:1612
17. Flach R, Hamilton DS, Selzer PM, Yen WM (1977) Phys Rev B 15:1248
18. Griesser HJ, Wild UP (1980) J Chem Phys 73:4715
19. Al'shits EI, Personov RI, Karlamov BM (1976) Chem Phys Lett 40:116
20. Suter GW, Wild UP (1988) Chem Phys 120:131
21. Volker S, Macfarlane RM (1979) IBM J Res Develop 23:547
22. Stoneham AM (1969) Rev Mod Phys 41:82
23. Kikas J, Ratsep M (1982) Phys Stat Sol (b) 112:409
24. Laird BB, Skinner JL (1989) J Chem Phys 90:3880
25. Loring RF (1990) J Chem Phys 92:1598
26. Simon SH, Dobrosavljević V, Stratt RM (1990) J Chem Phys 93:2640
27. Root LJ, Stillinger FH (1990) Phys Rev B 41:2348
28. Root LJ (1990) J Chem Phys 93:4364
29. Laird BB, Skinner JL (1989) J Chem Phys 90:3274
30. Kubo R (1962) J Phys Soc Jpn 17:1100
31. Gradshteyn IS, Ryzhik IM (1965) Table of integrals, series and products. Academic Press, New York
32. Abramowitz M, Stegun IA (1972) Handbook of mathematical functions. Dover, New York
33. Hansen JP, Verlet L (1969) Phys Rev 184:151